American Journal of
Biomedical Science & Research

www.biomedgrid.com
ISSN: 2642-1747

Review Article

Feasibility Study on the N-IORT® Adjuvant Treatment of Brain and Breast Cancers by Fast Neutrons Produced by a Compact DD- Fusion Generator

Maurizio Martellini[1*], Massimo Sarotto[2], Ka-Ngo Leung[3], Giuseppe Gherardi[1] and Lidia Falzone[1]

[1]*TheranostiCentre S.r.l., Via Freguglia 8-20122 Milan (ITALY)*

[2]*ENEA NUC-ENER-PRO, C.R. Saluggia, Strada per Crescentino 41-13040 Saluggia (ITALY)*

[3]*Berkion Technology LLC, Colusa Avenue 1102-94707 Berkeley (CA, USA)*

***Corresponding author:** Maurizio Martellinia, TheranostiCentre S.r.l., Via Freguglia 8-20122 Milan, ITALY.

To Cite This Article: *Maurizio Martellini*, Massimo Sarotto, Ka-Ngo Leung, Giuseppe Gherardi and Lidia Falzone, Feasibility Study on the N-IORT® Adjuvant Treatment of Brain and Breast Cancers by Fast Neutrons Produced by a Compact DD-Neutron Generator. Am J Biomed Sci & Res. 2024 22(3) AJBSR.MS.ID.002969,* DOI: 10.34297/AJBSR.2024.22.002969

Received: : April 26, 2024; **Published:** May 08, 2024

Abstract

This article describes the most significant outcomes of a 5-year collaborative research study on the intra-operative radiotherapy (IORT) with fast neutrons: the so-called neutron-IORT (nIORT®) technique. The fast neutrons of 2.45 MeV energy-produced by a compact generator through the deuterium-deuterium (DD) fusion reaction-should result very effective in cancer cells killing (via necrosis and apoptosis processes) mainly because of their high linear energy transfer (LET), very high relative biological effectiveness (RBE, about 16 times higher than X-rays and electrons used in standard radiotherapy (RT) and IORT treatments) and reduced oxygen enhancement ratio. The firsts two prototypes of the DD compact generator-limited in size and weight (~120kg), self-shielded and manageable remotely by a robotic arm - are currently under experimental characterisation. The second prototype foresees some technological advancements making possible its potential installation in an operating room dedicated to nIORT® treatments without posing any safety and environmental concern.

Accurate Monte Carlo calculations - modelling the DD compact generator equipped with the typical IORT applicators to be inserted in the surgical cavity and simulating the nIORT® irradiation treatments of breast and brain cancers-demonstrated that the apparatus can produce a fast neutron flux ~10^8 cm^{-2} s^{-1} and could administer equivalent dose rates ~2-5 Gy (RBE)/min in the tumour bed. Thus, it would be possible to administer very high dose targets in limited treatment times: e.g., a few minutes for the clinical endpoints foreseen by the standard RT and IORT protocols (~10-20 Gy (RBE)). Furthermore:

a. the rapid decrease in tissue depth of the dose gradient (within few centimetres) should avoid any adverse effect on normal tissues and the neighbouring organs

b. the near - isotropic neutron beam should permit to irradiate tumour beds with significant topographic irregularities - a therapeutic challenge with existing IORT technologies-and the bed margins (normally filled by quiescent cancer cells) with potential benefits for the tumour local control.

c. Despite the almost-isotropic neutron emission by DD fusion reactions, different nIORT® applicator shapes (and sizes) lead to different figures of merit for the most common dosimetry parameters. The Monte Carlo simulations performed with 4-cm-diameter cylindrical and hemispherical applicators demonstrated that:

d. the cylindrical shape - here considered for the brain cancers treatment with craniotomy - supplies a front-focused dose distribution, with a very high dose rate (≅5 Gy (RBE)/min in the centre of the tumour bed and limited dose rates in the tissue on the lateral side of the applicator (i.e., skull and skin)

e. the hemispherical shape - here considered for the breast cancers treatment-supplies an almost iso - dose distribution with dose rate levels of ≅2 Gy (RBE)/min.

The authors' idea is that the "physical - biological" features of the fast neutron beam - such as high RBE and near - isotropic emission, combined with the possible choice between the front - focused and iso-dose spatial distributions - could contribute to enhance the eligibility of IORT treatments for solid cancers, by satisfying the usual requirements in common clinical practice for the selection of the most suitable technique which needs a thoughtful balancing between the aimed local control of the tumour and the adverse effects of the radiation on normal tissues.

List of Abbreviations: BNCT: Boron Neutron Capture Therapy; CNG: Compact Neutron Generator; DD: Deuterium-Deuterium; DSB: Double Strand Break; EBRT: External Beam Radiotherapy; EMT: Epithelial-Mesenchymal Transformation; GBM: Glioblastoma Multiforme; HDPE: High Density Polyethylene; HR: Homologous Recombination; ICI: Immune-Checkpoints Inhibitor; IORT: Intraoperative Radiation Therapy; IOERT: Electron IORT; IOHDR: High-Dose Rate Brachytherapy; IR: Ionizing Radiation; LET: Linear Energy Transfer; LEX-IORT: Low Energy X-rays IORT; LTC: Local Tumor Control; MCNP: Monte Carlo N-Particle; NHEJ: Nonhomologous End Joining; nIORT®: Neutron IORT; OAR: Organ at Risk; OER: Oxygen Enhancement Ratio; OR: Operating Room; QCC: Quiescent Cancer Cell; RIAE: Radiation-Induced Abscopal Effect; RIBE: Radiation-Induced Bystander Effect; RISM: Radiation-Induced Secondary Malignancy; RT: Radiation Therapy; SSB: Single Strand Break; TME: Tumor Microenvironment; TMZ: Temozolomide; TT: Treatment Time.

Symbols:

$D'_{f,(n,\gamma)}$: Physical dose rate due to neutrons or photons (n, γ) [Gy min-1]

$D'_{eq,(n,\gamma)}$: Equivalent dose rate due to neutrons or photons (n, γ) [Gy (RBE) min-1]

$D'_{eq,tot}$: Equivalent dose rate due to neutrons and photons (n+ γ) [Gy (RBE) min-1]

$D_{eq,tot}$: Equivalent dose due to neutrons and photons (n+ γ) [Gy (RBE)]

D_{Target}: Target dose / Clinical endpoint [Gy (RBE)]

Φ_n: Neutron flux [cm^{-2} s^{-1}]

Φ_γ: Photon flux [cm^{-2} s^{-1}]

TT: Treatment Time

Min: minute(s)

Introduction

The radiation therapy (RT) treatments of solid cancers after the maximal safe surgical resection are common in guideline recommendations: they aim to maximize the local tumour control (LTC) leading to some benefits in overall survival and progression-free survival times of patients affected by high-grade tumours and possible metastases. The ionizing radiation (IR) particles produced by the RT devices causes the death of tumour cells in target tissues by inducing DNA damages - as abasic sites, single-strand break (SSB) and double-strand breaks (DSBs): damages are caused either directly by the ionization track of the incident radiation or indirectly by oxidative stress phenomena generating reactive oxygen species as free radicals, also affecting the tumour immune response [1].

With the most recent technological advancements, the intra-operative radiotherapy [2] (IORT) has emerged as a very promising adjuvant treatment with several studies demonstrating both feasibility and outcome equivalence, if not superiority when applied in the optimal setting, respect to the external beam radiotherapy (EBRT) [3]. In the IORT treatment plannings, the dose target is administered in one-shot irradiation directly in the "open wound" surgical cavity (and not by fractionation scheduled EBRT on the skin upon the "closed wound") and the zeroing of the time to initiation limits the repopulation of residual cancer cells in the tumour microenvironment (TME).

In this feasibility study, the IORT treatment of the primary breast and brain tumours - with possible local recurrences - was considered. The breast's carcinomas are probably among the most diffuse tumours worldwide and the brain tumours, such as the glioblastoma multiforme (GBM) representing one of the most aggres-

sive primary cancers with an average survival time of 6÷18 months. The most recent IORT techniques have been already adopted for the treatment of both breast [4] and brain [5] tumours, aiming to avoid the tumour cell proliferation between surgery and radio-chemotherapy and to spare healthy tissues. A significant effort was devoted toward the GBM treatment: since this neoplastic tissues grow slowly, local recurrence is the major cause for clinical deterioration (and deaths) and is frequently observed within 2÷3 cm from the initial lesion, the one-shot IORT irradiation - with craniotomy after maximal surgical resection - represent a very promising therapeutic option [6,7].

The current IORT techniques for the solid cancers' treatment exploit as IR particles low-energy (~50 keV) X-rays - with the so-called low energy X-rays IORT (LEX-IORT [8]) - and high-energy (~5÷10 MeV) electrons (IOERT [9,10]). The high-dose rate brachytherapy (IOHDR [11]), relying on a sealed radionuclide source being placed within the tumour resection cavity (e.g., ^{252}Cf needles), may also be applied for very small target volumes. In the breast cancer treatment, the IORT technique avoids irradiation of normal tissues - such as skin, heart, lungs, ribs and spine - and some clinical trials shown to improve cosmetic outcome when compared with EBRT [4]. Similarly, for the brain malignancies, the IORT treatments present radiobiological factors inducing favorable outcome data beyond those obtained with standard techniques [12,13]. But, in spite of these promising outcomes and some significant advantageous aspects with respect to the EBTR, the standard IORT techniques still present some limitations such as:

1) the tumour beds with significant extension and topographic irregularities, that remain a therapeutic challenge with existing technologies foreseeing a focused beam (as in IOERT, most reliable for flat tissue surfaces) and/or a "limited" target area for the beam (as in LEX-IORT);

2) the low linear energy transfer (LET) of the photon and electron IR in biological tissues, that induces mainly isolated lesions as DNA SSBs. Otherwise, IR particles with high LET would induce more highly localized DSBs and clustered DNA damage more difficult to repair, leading to necrosis and apoptosis of the cancer cells [14,15].

By exploiting the beneficial peculiarities of the IORT technique - i.e., time to initiation zeroing, high dose levels administered in the "open wound" tumour bed and reduced levels in neighbouring normal tissue - these limitations could be overcome using the fast neutrons as IR particles [15-17]. This feasibility study refers to the so-called neutron-IORT (nIORT®) technique [18], invented by the TheranostiCentre S.r.l. company (TC, Italy) and further developed in collaboration with the Berkion Technology LLC company (BT, USA) and the Italian National Agency for New Technologies, Energy and Sustainable Economic Development (ENEA).

The 5-year research activities on nIORT® led to the fabrication of the first two prototypes of a compact neutron generator (CNG [19]) that, through the deuterium-deuterium (DD) fusion reaction, produces neutrons of 2.45 MeV energy. The CNG is self-shielded, limited in size and weight (~120 kg) and can be operated remotely by a robotic arm. The second prototype foresees some technological advancements making possible its potential installation in an operating room (OR) dedicated to nIORT® treatments without posing any safety and environmental concern [20]. The experimental research program on nIORT® is currently ongoing and the irradiation performances of the two CNG prototypes - e.g., for *in vitro* tests on commercial cancer cells - are going to be performed in a new equipped ENEA laboratory [21].

As described below, the nIORT® irradiation could allow solid cancers' adjuvant treatment mainly because:

1. The high flux level of fast neutrons (~10^8 cm^{-2} s^{-1}) produced by the DD-CNG;

2. the high LET (~40keV/μm as average [22], or even higher [23]) and the very high relative biological effectiveness (RBE) of fast neutrons (≅16 at 2.45MeV energy [24]), coupled with the rapid attenuation of the physical (and equivalent) dose in tissues depth which should spare the normal tissues around the tumor bed and the neighbouring organs at risk (OARs);

3. the diffuse spatial dose distribution of the neutron beam in the irradiated target area, which is well suited for extended and irregular tumor bed tissues [20];

4. the reduced oxygen enhancement ratio (OER [25]), that is less affected by a hypoxic TME in case of neutrons and the nIORT® monoenergetic spectrum would set the OER to a plateau of ≅1.45 [26].

Different from boron neutron capture therapy (BNCT [27]) exploiting thermal and epithermal neutrons to induce (n, α) reactions in boron carriers injected into the patients, the fast neutrons produced by the CNG interact directly and efficiently with the hydrogen nuclei, producing recoil protons that ionize the tissues. The high LET and, mostly, the very high RBE-that at 2.45MeV energy is 16 times higher than X-rays and electrons used in standard RT and IORT treatments-which is very effective in cancer cell killing through highly localized DSBs and clustered DNA damages [28]. At the same time, difficulties and limitations of the irradiation treatments made in the past with fast neutrons17 are mainly overcome by the IORT modality. The utilization of a compact source, instead of big facilities such as nuclear reactors or high energy accelerators, represents a fundamental advantage in the view of possible treatments in a hospital OR.

The near-isotropic neutrons emission produced by the CNG has the important advantage of being less sensitive to the margins of the surgery cavity and to the possible intra-tumour heterogeneity of the tumour cells. The neutron beam behaves like an IR "foam" filling the surgical cavity and allows to irradiate the tumour bed margins, normally filled by potential quiescent cancer cells (QCCs), with lower - but still significant - dose levels. Thus, potentially, the almost "spherically symmetric" beam - a peculiarity of the "not-charged-not-focused" neutron particles - should allow to improve the LTC through the reduction of local recurrences and metastasis in the TME and, at the same time, to avoid adverse effects of too high dose levels administered in the surrounding normal tissues.

In this article the nIORT® potential benefits were investigated in the view of the brain and breast tumors' treatment by means of the Monte Carlo N-Particle (MCNP) ver. 6.1 code [29]. The MCNP simulations - modelling accurately the CNG equipped with the typical IORT applicator to be inserted in the surgical cavity - were performed by two nIORT® applicators of 4 cm in diameter and different shapes:

a) a hemispherical one allowing to an almost iso-dose distribution in the surgical cavity, here adopted for the irradiation of the breast tumour bed;

b) a cylindrical one allowing to a more front-focused dose distribution in the surgical cavity, here adopted for the irradiation of the breast tumour bed with craniotomy, trying to minimise the dose levels in surrounding-lateral skull and skin normal tissues.

It should be noted that this research study deals only with the radiological aspects associated with the nIORT® irradiation of head and trunk tissues, but it does not deal with any other relevant clinical issues related to the specific cancer pathology. The MCNP simulations demonstrated that the CNG-nIORT® device operated at 100 kV-10 mA DC can deliver equivalent dose rates ~2÷5 Gy (RBE)/min in the tumour bed. Thus, it could administer the clinical endpoints foreseen by the standard IORT protocols (~10-20 Gy (RBE)) in treatment times of few minutes, by providing a sort of "switching on and off neutron brachytherapy tool" but avoiding the insertion (and maintenance) of needles of instable radioisotopes into patients.

The D-D Fusion Compact Generator for nIORT®

The first two CNG prototypes - designed and developed in the collaborative research program by TC, BT and ENEA - were fabricated in the BT laboratories in the last two years. The CNG design was filed as an international patent in 2021 and registered at the WIPO (World Intellectual Property Organization) in 2023 [30]. The second CNG prototype was recently fabricated with some technical advancements - such as operation reliability, safety, and radiation protection aspects - that should make the apparatus suitable to be installed in an OR dedicated to nIORT® treatments, without posing any safety and environmental concern.

The conceptual scheme in Figure 1 summarises the advantageous design features of the DD-CNG and shows its main three components:

1) the ion source, that is a RF-driven plasma chamber with D (a nonradioactive isotope of hydrogen);

2) the acceleration column made of High-Density Polyethylene (HDPE, having excellent properties in shielding neutrons);

3) the beam target electrode made of titanium.

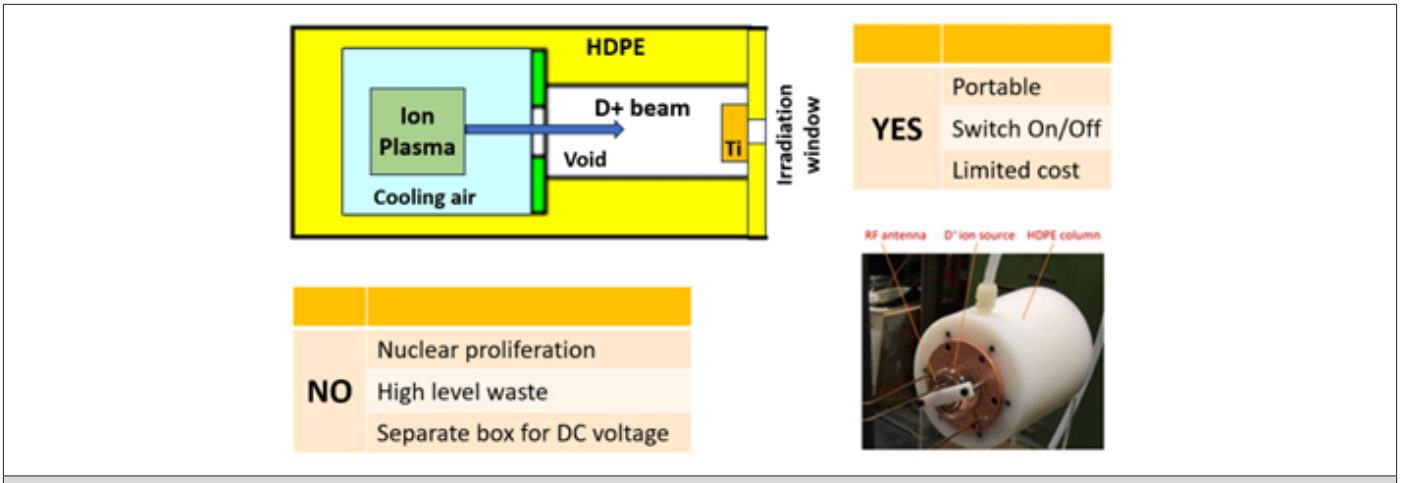

Figure 1: Conceptual design and main features of the D+ ion-based CNG. Picture of the HDPE accelerator column with the D+ ion source plasma chamber (right-bottom).

The picture in the right-bottom part of Figure 1 shows the HDPE accelerator column (about 15 cm in diameter) and the RF plasma chamber attached to it. The positive deuterium ions (D+) created in the plasma chamber are accelerated to the titanium target where 2.45MeV neutrons are produced by the DD fusion reaction. Operating the DD-CNG at 100 kV-10 mA DC, a neutron yield of 3.3 10^9 s^{-1} is generated in the titanium target and a neutron flux of ~10^8 cm^{-2} s^{-1} at the irradiation window close to the target [31, 32].

The Monte Carlo analyses described here are based on the CNG design equipped with the typical IORT applicator to be inserted in the surgical cavity instead of the irradiation window for materials irradiation purposes (as in Figure 1 for e.g., in vitro tests). The nIORT® applicators chosen for this study are 4 cm in diameter and made of lucite ($C_5O_2H_8$, almost transparent for neutrons) that, via hard-docking, can be inserted close to - or in contact with - the tumour bed in the surgical cavity. In this study, the cylindrical and hemispherical shapes were considered for the brain and breast nIORT® irradiation, respectively: in the past, some MCNP analyses were performed by using cylindrical applicators of different diameters [20,33].

The left side of Figure 2 shows a 2D section of the MCNP model of the CNG and surrounding shields, made of borated PE and an external layer of lead (mainly for γ rays). The whole system is a cylinder with about 30cm in diameter and 40cm in length. The right frame of Figure 2 shows an enlarged drawing of the MCNP model of the 4-cm-diameter hemispherical applicator. The hemispherical

lucite surrounds a HDPE bearing-ledge structure containing an aluminium holder for the titanium target. The ion source chamber (in the back part of the acceleration column, see Figure 1) was not modelled in MCNP: this simplification has no impacts on the flux and dose rate results into the biological tissues, since the simulations start from the (near-isotropic) spatial distribution of the 2.45MeV neutrons emitted from the titanium target on the opposite side of the CNG.

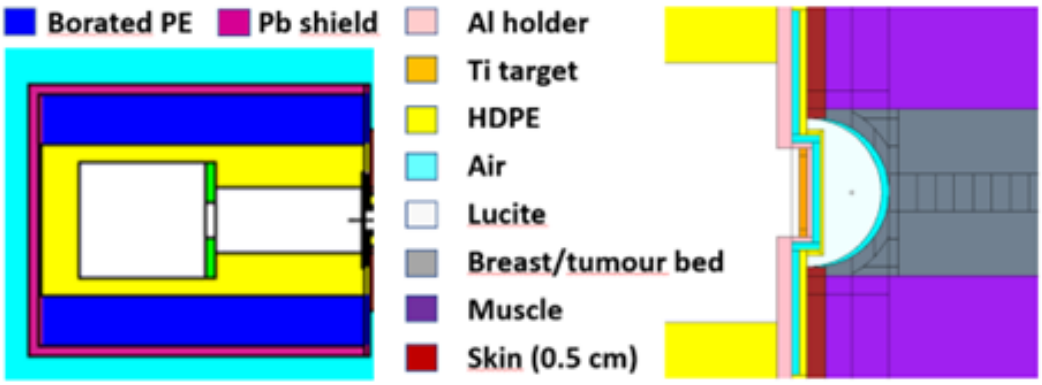

Figure 2: Vertical section of the MCNP model of the CNG and surrounding shields (left). Zoom section of the MCNP model of the hemispherical nIORT® applicator inserted in the breast surgical cavity (right).

As shown in the right side of Figure 2, the nIORT® applicator positioned in the breast surgical cavity is surrounded by covering skin (0.5cm thick i.e., > 0.3cm to consider "folds") and muscle tissues. Obviously, the tumour bed margins are not so well defined as in the MCNP model (with a net separation between the breast tumour bed and normal muscle tissues as in Figure 2). In any case, the dose rate levels were accurately calculated in small volumes for all surface tissues of the surgical cavity, and in deep breast tissues.

Methodology

The Monte Carlo simulations were performed by means of the MCNP ver. 6.1 code [29] coupled with the most up to date ENDF/B-VIII.0 nuclear data [34]. The neutron flux levels in the surgical cavity were evaluated starting from the neutron yield (≅ 3.3 10^9 s^{-1}) generated by the 100kV-10 mA DC D^+ ions impinging on the titanium target, with a near-isotropic direction of emission reproduced accurately with the code. The simulations were not restricted to neutrons (i.e., primary ones coming from the titanium target and secondary ones coming from the scattering with CNG components and patient tissues), but they also include the photons: i.e., gammas (γ) created by neutrons interaction with matter. The physical (Gy) and equivalent (Gy (RBE)) dose distributions in the biological tissues of the surgical cavity around the applicator were then evaluated from neutron and photon flux levels.

Starting from the physical dose rates (Gy/min) due to neutrons ($D'_{f,n}$) and gammas ($D'_{f,\gamma}$) calculated "directly" by MCNP, the total equivalent dose rate ($D'_{eq,tot}$; Gy (RBE)/min) administered can be obtained by the following equation:

$$D'_{eq,tot} = D'_{eq,\gamma} + \int W_R(E) D'_{f,n}(E) dE \ \text{[Gy (RBE)/min]} \qquad (1)$$

where:

i) "$W_R(E)$" is the radiation weighting factor for neutrons in human tissues (≅16 at 2.45 MeV24);

ii) the radiation weighting factors for photons is one (i.e., $D'_{eq,\gamma} \equiv D'_{f,\gamma}$).

Actually, the neutrons contribution to the total dose rate [1] results three orders of magnitude higher than the gamma ones because of the higher neutron flux (≅20x photon flux), LET (≥5x photon LET) and RBE (≅16x photon RBE). The equivalent dose due to neutrons was calculated starting from the flux and physical dose spectra evaluated by MCNP in the biological tissues and the corresponding weighting factor W_R, whose behavior with energy was accurately interpolated by a linear fit of 13 energy groups [32].

Referring to the aimed dose target (D_{Target}) defined by standard clinical protocols, usually named clinical end point, the required Treatment Time (TT) can be easily obtained:

$$TT = D_{Target} / D'_{eq,tot} \ \text{[min]} \qquad (2)$$

The spatial distributions of the equivalent dose rates (1) in the surgical cavity were accurately evaluated by MCNP to estimate the peak value administered in surface tissues at the centre of the tumour bed - usually corresponding to the D_{Target} clinical end point- as well as the dose administered in the surrounding tumour bed margins and normal tissues (into and around the surgical cavity), whose compositions were retrieved from reliable MC human phantoms' models in literature [35].

Dose Rate Levels in Breast Surgical Cavity

As shown in the right side of Figure 2, the surface tissues of the breast surgical cavity were modelled in MCNP with cells of different shapes (≅2÷5 mm thick). The cells numbering adopted in MCNP is shown on the left side of Figure 3: the surface tissues of the breast tumour bed are represented by the dark grey cells 301, 322, 323 and 324, surrounded by the dark red cell 325 representing the nearest surrounding skin. The graph in the right frame of Figure 3 shows the dose rate values obtained in these superficial cells: the "R" horizontal axis represents the distance between the centre of the tumour bed and centers of each surface cell around the hemispherical nIORT® applicator. In the left frame, the light grey cell 39 represents the lucite applicatorand the light blue cell 38 represents the air gap between the applicator and the surgical cavity, to model (at some extent) the not uniform contact between the applicator and the tissues.

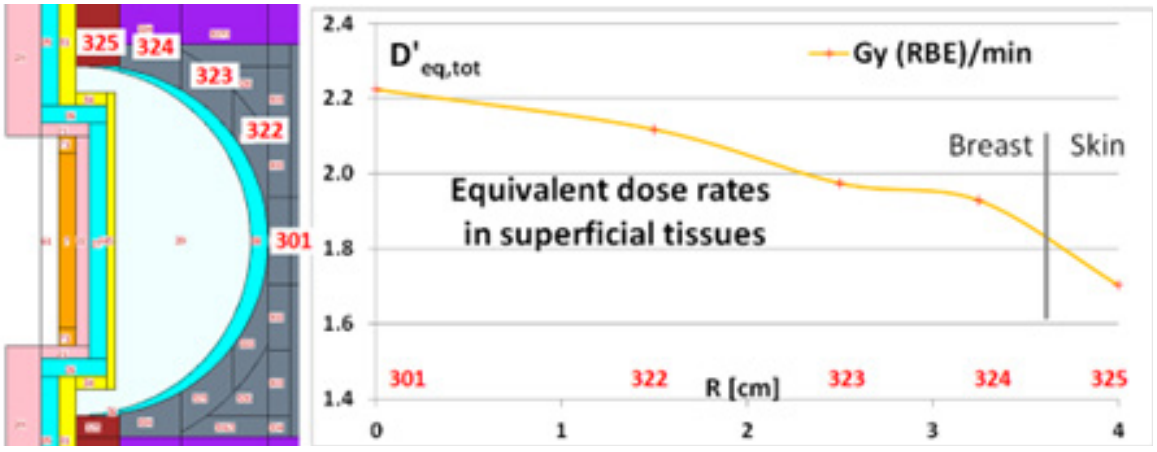

Figure 3: Zoom section of the MCNP model of the 4-cm-diameter nIORT® hemispherical applicator inserted in the breast surgical cavity (left: red numbers refer to MCNP cells). MCNP results for equivalent dose rates in surface tissues of the surgical cavity (right).

As shown in the right side of Figure 3 and in Table 1, an equivalent peak dose rate of ≅ 2.2 Gy (RBE)/min is administered in the tumour bed centre (cell 301) and quite high dose rates (≅ 2.0 Gy (RBE)/min) are maintained in the whole tumour bed (cells 322, 323, 324), while lower values (≅ 1.7 Gy (RBE)/min) are administered in the surrounding skin (325) tissues. As a Monte Carlo code, MCNP is affected by the statistical noise of the results due to its stochastic nature. For easiness, the uncertainty of the dose rate results is not indicated in the graph and table: their relative standard deviation is however less than 1%.

Figure 4 shows the equivalent dose rate profiles in breast depth: the dose rates were sampled with 0.25÷0.5 cm thick cells (1 cm in radius) along the symmetry axis of the applicator. The dose level drops rapidly decreasing by a factor 2 at ≅1cm depth and by a factor 5 at ≅2.5cm. Hence, the overwhelming part of the dose is administered in the surface tissues of the surgical cavity and quite high doses are released until about 1cm depth. Beyond that it decreases rapidly avoiding an "excessive" irradiation of normal breast tissues and closest OARs.

Table 1: Equivalent dose rates in surface tissues of the breast surgical cavity (MCNP results with 4-cm-diameter hemispherical nIORT® applicator).

Dose Rate	Tumour Bed			Skin
	Peak	Average	Minimum	Peak
Gy (RBE)/min	2.2	2.0	1.9	1.7

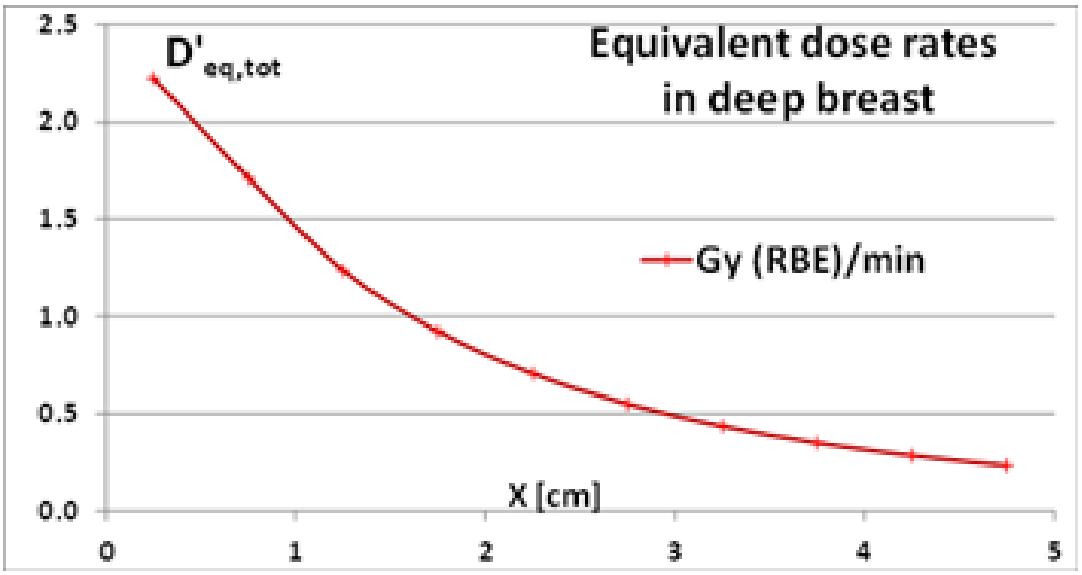

Figure 4: Equivalent dose rate profiles in breast depth (MCNP results for 4-cm-diameter hemispherical nIORT® applicator).

Dose Rate Levels in Brain Surgical Cavity

The main figures of merit obtained by MCNP with a 4-cm-diameter cylindrical nIORT® applicator for the brain cancer treatment have already been published [33]: they can be briefly summarized for completeness and a comprehensive comparison with the hemispherical applicator's performances. Figure 5 shows the MCNP model of the CNG equipped with the cylindrical applicator (in purple) and the surrounding brain surgical cavity (dark grey),

skull (light grey) and skin (dark red) tissues. The left side of Figure 6 reports the MCNP cell numbering adopted for the surface tissues modelled with 2.5 mm thick cells in cylindrical shell shape. The graph in the right side of Figure 6 shows the equivalent dose rate values obtained in these superficial cells: the "R" horizontal axis represents the distance between the centre of the tumour bed and centers of each cell representing surface tissues. With the cylindrical geometry, R coincides with the radius of the applicator end-cap until 2cm, while bigger values refer to the skull and skin cells on its lateral side.

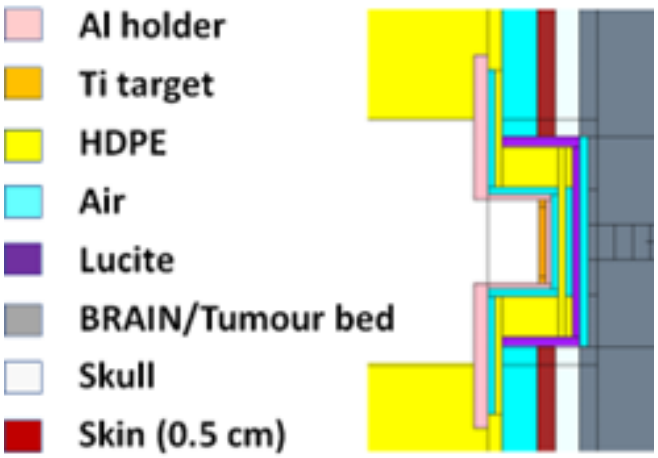

Figure 5: MCNP model of the 4-cm-diameter nIORT® cylindrical applicator inserted in the brain surgical cavity.

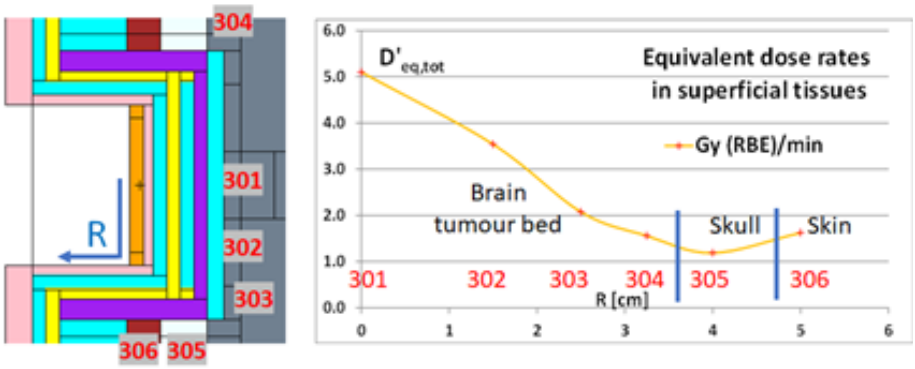

Figure 6: Zoom section of the MCNP model of the 4-cm-diameter nIORT® cylindrical applicator inserted in the brain surgical cavity (left: red numbers refer to MCNP cells). MCNP results for equivalent dose rates in surface tissues of the surgical cavity (right [33]).

As shown in the right frame of Figure 6 and reported in Table 2, the dose rate peak in the centre of the tumour bed reaches ≅5 Gy (RBE) / min, the average/minimum dose rates in the surface tissues of the whole tumour bed result 2.5/1.6 Gy (RBE) / min, respectively, while the maximum dose rate levels in skull and skin result 1.2 and 1.6 Gy (RBE) / min, respectively. The decrease of the equivalent dose rates in brain depth (here not shown) is very similar to the behavior of Figure 4 for the brain tissues (i.e., dose levels drop rapidly by a factor 2/5 at ≅1/ ≅2.5cm depth, respectively).

Table 2: Equivalent dose rates in surface tissues of the brain surgical cavity (MCNP results with 4-cm-diameter cylindrical nIORT® applicator [33]).

Dose Rate	Tumour Bed			Skull	Skin
	Peak	Average	Minimum	Peak	Peak
Gy (RBE)/ min	5.1	2.5	1.6	1.2	1.6

The nIORT® Beam Features

The choice of the most eligible IORT adjuvant treatment for local cancer metastases after surgical rejection is strictly related with the tumour bed (and patient) conditions: depending on the volume, location and sensitivity of the tumour and the surrounding normal tissue, different techniques may be selected. Among the current IORT techniques, the IOERT has been demonstrated to be feasible and effective in LTC of disease in breast, pancreas, soft tissue sarcomas, head and neck, uterine, and colorectal cancers: even if structural limitations of the cylindrical applicator tube have restricted use to cavities with clear line-of-sight parameters, some experiences describing an intracranial use in high-grade glioma were published [9]. Otherwise, the LEX-IORT devices with small spherical applicators allow for a more suitable adaptation to the small surgical cavities, as the brain resection cavity walls [8].

Despite the absence of experimental data and clinical evidence, the dosimetry parameters calculated by MCNP in the biological tis-

sues irradiated by fast neutrons can be "qualitatively" compared with those produced with the existing IORT technologies [36]. For a proper comparison among the different options and the subsequent choice of the most eligible treatment, the physical features of the IR particles - and their biological effects in the irradiated tissues - must be considered.

To reach high dose rates, besides the flux level of IR particles in the tumour bed (proportional to the beam power), the type of IR used represents a key factor. The low-LET IR (as X-rays) induces simple DNA lesions that are quite efficiently repaired by cancer cells, whereas high-LET radiation causes complex DNA lesions difficult to repair [37]. Indeed, the high LET and very high RBE of fast neutrons (≃16 at 2.45 MeV, i.e., 16 times higher than the photons and electron unitary values) should induce the necrosis of the cancer cells cycles in the shortest possible time compared to their repopulation and redistribution times. The cells damage is more dispersed and uniform with low-LET IR and more discrete, clustered, and heterogeneously scattered along the beam tracks with high-LET particles [38].

Thus, potentially, the adjuvant nIORT® treatment adopting fast neutrons could be a very effective therapeutic option for the most severe solid tumours since the high LET-RBE neutron particles should be very efficient in cancer cell killing. Of course, this "extremely beneficial" feature of the neutron beam with 2.45 MeV energy will have to be validated experimentally, e.g., by irradiating with the CNG-nIORT® device an anthropomorphic water phantom endowed with vials.

Furthermore, the almost-isotropic spatial distribution of the neutron beam permits to irradiate large target area including the tumour bed margins and the TME, as indicated by several studies with the MCNP code [20,31,32,33]. By referring the CNG design equipped with a 4-cm-diameter hemispherical applicator, Figure 7 shows the computed 2D maps of the neutron flux distributions (in cm^{-2} s^{-1}) inside the IORT applicator and in the biological tissues of the surrounding breast surgical cavity. It can be clearly seen that the near-isotropic neutrons diffusion permits to irradiate large tissue areas with quite-high uniform dose levels in the tumour bed surface and, aiming the LTC, with lower dose values administered in the tumour bed margins and surrounding normal tissues. For this peculiar aspect, the nIORT® could potentially represent a unique therapeutic option for the LTC aiming the "near-total" disappearance of metastases by limiting any local recurrence after the treatment.

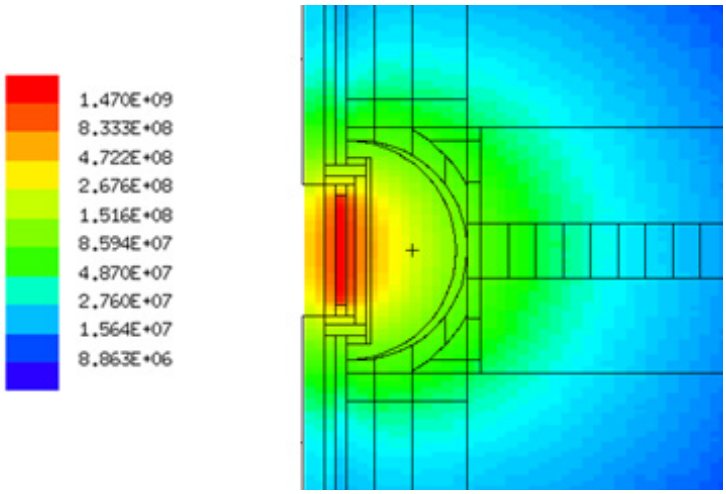

Figure 7: 2D neutron flux spatial distributions inside the 4-cm-diameter hemispherical nIORT® applicator and in the surrounding breast surgical cavity (MCNP: cm^{-2} s^{-1}).

By comparing the 2D flux distribution in Figure 7 with the equivalent dose profile in tissues depth of Figure 4, it can be deduced that the neutrons diffuse into tissues but, because of their high LET-RBE, the overwhelming part of the dose is released at surface and in the first 1÷2 cm depth. The deep tissues are still irradiated by the thermal and epithermal tails of the neutron flux having decisively lower LET and RBE values, and hence significantly less effective in cells damaging by sparing normal tissues and the neighbouring OARs.

Even if the neutrons direction of emission from the titanium target (see Figure 1) is almost isotropic, the dose spatial distributions in the surface tissues of the surgical cavity result to be remarkably different with the cylindrical (Figure 6) and hemispherical (Figure 3) applicator shapes. To compare the two dose rate profiles, the dose rate ratios between:

i) the average and minimum values in the tumour bed, the maximum values in normal tissues;

ii) the peak value in the tumour bed centre.

were evaluated for both hemispherical and cylindrical nIORT® applicators. These dose rate ratios, reported in Table 3, indicate that:

a) the hemispherical shape provides an almost iso-dose distribution in the surgical cavity with average (in the whole tumour bed) and minimum (at bed margins) dose levels approximatively at about 91% and 86% of the peak administered in the tumour bed centre;

b) the cylindrical shape provides a more front-focused distribution in the surgical cavity with the average (in the whole tumour bed) and minimum (at bed margins) dose levels approximatively at about 50% and 30% of the peak in the tumour bed centre.

The results in Table 3 summarises with few parameters the difference between the dose spatial distributions obtained by the two nIORT® applicator shapes and indicated that:

a) the hemispherical applicator with an almost iso-dose beam could be more suitable for the treatment of breast cancers, in which a uniform dose distribution is usually required in the whole surgical cavity;

b) the cylindrical applicator with a front-focused beam could be suitable for the treatment of brain cancers, by minimizing the doses administered to brain, skull, and skin normal tissues.

Table 3: Equivalent dose rate ratios (fraction of the peak) in surface tissues of surgical cavities (4-cm-diameter hemispherical and cylindrical nIORT® applicators).

Applicator Shape (organ)	Tumour Bed /Peak			Skull / Peak	Skin / Peak
	Peak	Average	Minimum		
Hemisphere (Breast)	1.0	0.91	0.86		0.77
Cylinder (Brain)	1.0	0.49	0.31	0.24	0.31

Potential nIORT® Treatment Plannings

The CNG performances for potential nIORT® treatment plannings were evaluated in view of possible clinical applications. By referring to the clinical endpoints defined in the standard IORT and EBRT protocols, the correspondent TT needed to administer such dose targets in a single session can be easily deduced by equation (2) from the equivalent dose rate results reported in Tables 1 and 2. Usually, in dependence of the tumour bed (and patient) conditions, two dose targets are conventionally adopted: the so-called Boost and Radical regimes foreseeing clinical endpoints of about 10-12 and 20 Gy (RBE), respectively [3].

Tables 4 and 5 report the irradiation performances of the CNG equipped with the 4-cm-diameter hemispherical and cylindrical nIORT® applicators, respectively. For the Boost and Radical regimes, 10 and 20 Gy (RBE) were assumed as dose targets for the peak value (in the centre of the tumour bed) and for the average value in the whole tumour bed. The TT foreseen with the hemispherical applicator is about two times the TT obtained with the cylindrical one, trivially because of the about half dose rate peak value. This difference is mainly due to the $1/r^2$ flux decrease: indeed, the resulting distance between the titanium target (origin of the 2.45 MeV neutrons) and the tumour bed results almost the double with the hemispherical shape.

Table 4: CNG irradiation performances for potential nIORT® treatments in Boost (10 Gy (RBE)) and Radical (20 Gy (RBE)) regimes (4-cm-diameter hemispherical applicator).

Dose target Gy (RBE)	Peak / Ave Criteria	TT [min]	Gy (RBE)			
			Tumour Bed			Skin
			Peak	Average	Minimum	Peak
10	Peak	4.5	10	9.1	8.6	7.7
	Average	5.0	11.0	10	9.5	8.5
20	Peak	9.1	20	18.2	17.3	15.5
	Average	10.0	22	20	19.0	17.0

Table 5: CNG irradiation performances for potential nIORT® treatments in Boost (10 Gy (RBE)) and Radical (20 Gy (RBE)) regimes (4-cm-diameter hemispherical applicator).

Dose target Gy (RBE)	Peak / Ave Criteria	TT [min]	Gy (RBE)				
			Tumour Bed			Skull	Skin
			Peak	Average	Minimum	Peak	Peak
10	Peak	2.0	10	4.9	3.1	2.4	3.1
	Average	4.0	20.4	10	6.4	4.8	6.4
20	Peak	3.9	20	9.8	6.3	4.7	6.3
	Average	8.0	40.8	20	12.8	9.6	12.8

In some details, the performances of the CNG-nIORT® device for potential treatment planning can be summarized as followed:

a. with the hemispherical applicator (Table 4), the peak / average dose target of 10 Gy (RBE) can be administered in about 4.5 / 5 min, respectively.

b. With the cylindrical applicator (Table 5), the peak / average dose target of 10 Gy (RBE) can be administered in about 2 / 4 min, respectively.

Trivially, the same proportions between TTs occur adopting 20 Gy (RBE) as dose target. It can be noticed that adopting the "av-

erage dose target criterion" in this Radical regime, the dose peak obtained with the front-focused cylindrical applicator reach about 41 Gy (RBE) in the tumour bed centre. This case can then be classified as belonging to the Ultra-Radical regime, as well as treatment plannings with higher clinical endpoints, as sometimes required in the most severe cases. The high dose rates allowed by the DD-CNG permit to administer much higher target in limited TTs (e.g., up to 50/75 Gy (RBE) in 10 / 15min with the cylindrical nIORT® applicator [33]).

It can be observed that, in the BNCT field, the 12.6 Gy (RBE) limit is usually assumed as peak dose for the normal tissues [39, 40]. In the dose regimes examined in Tables 4 and 5 this threshold limit in healthy skin (and skull) tissues results:

i) largely exceeded with the hemispherical applicator in the 20 Gy (RBE) Radical regime (see last two rows of Table 4);

ii) slightly exceeded with the cylindrical applicator only by adopting 20 Gy (RBE) as average dose target in the whole tumour bed (see last row of Table 5).

Discussion

As evident from the results of Tables 3÷5, the applicator shape directly impacts both the equivalent dose rate level and its spatial distribution in the surface tissues of the surgical cavity (despite the almost-isotropic neutrons emission). In some details:

1) the cylindrical applicator - here applied for the brain tumour irradiation (with craniotomy) - supplies a front-focused dose distribution with:

1. a) a very high dose rate (≅5 Gy (RBE)/min in the centre of the tumour bed), essentially due to the very short distance between the tumour tissues and the Ti target source;

1. b) limited dose rateslimited dose rates in the tissue on the lateral side of the applicator (i.e., skull and skin) at about 12% of the peak administered in the tumour bed centre).

2) the hemispherical applicator - here applied for the breast tumour irradiation - supplies an almost iso-dose distribution with:

2. a) the dose rates in the tumour bed centre "limited" to ≅2Gy (RBE)/min, for the increased distance of irradiated tissues from the titanium target;

2. b) the dose rates at the margins of the tumour bed and skin respectively at 87% and 77% of the peak administered in the tumour bed centre.

The choice of cylindrical and hemispherical nIORT® applicators lead to different TTs (about the half with the cylindrical shape) and different beam features, with more front-focused or iso-dose spatial distributions in the surgical cavity. This possible choice has the great potentiality to satisfy the usual requirements in common clinical practice for the selection of the most eligible IORT technique, requiring an appropriate balancing between the aimed LTC and, at the same time, the adverse effects of the radiation on normal tissues.

It must be also remarked that the dosimetry parameters obtained by MCNP refer to:

i) the brain and breast cancers treatment, but the results could be generalized to the treatment of other solid tumours with both cylindrical and hemispherical nIORT® applicators. For more accurate dose levels and spatial distributions, the topography of the specific organs/tissues into (and around) the surgical cavity should be properly modelled.

ii) the nIORT® applicators with 4cm in diameter. Different sizes could be employed by obtaining slightly different figures of merit. However, 4 cm is close to the minimum diameter allowed by the CNG design. Otherwise, diameters larger than 4cm can be easily fabricated: with the cylindrical shape, the dose rate in the tumour bed centre will remain the same (5 Gy (RBE)/min) and will be lower in tissues on the lateral side of the applicator. As an example, with a 6-cm-diameter size, the dose levels in skull and skin in a nIORT® brain treatment are at about 9%÷12% of the peak [33], respectively, instead of 20÷30% obtained with the 4-cm-diameter applicator. Even if easily fabricable, since the applicator is rigid it would be challenging to adopt larger diameters for brain cancers treatment (with craniotomy), and more generally, for other difficult achievable body parts such as pelvis and narrow cavities.

The physical and dosimetry parameters obtained by the MCNP simulations pointed out that some significant benefits should derive from the high LET-RBE values of fast neutrons, independently from the shape (and size) of the nIORT® applicator chosen. In some details these potential advantages can be summarized as follows.

1) With a high flux of fast neutrons impinging directly on the tumour bed, the irradiation is focused on the tumour volume with minimal normal tissue injury. The high LET-RBE neutrons yields a rapid dose gradient in tissues depth (see Figure 4: the overwhelming part of the nIORT® dose is administered in the superficial tissues and in the first cm depth, while in deeper tissues the levels are decisively lower: ≅1/5 at 2÷2.5cm depth). For the LTC in metastatic tumour cavities, this dose profile can provide maximal dose to non-visualized microscopic disease but, on the contrary, rapid dose decrements can allow for under treatment of residual disease. However, since the nIORT® dose gradient in tissue depth results not steep as in the LEX-IORT techniques (and less smooth than in the IOERT ones [33]), the under treatment of residual disease should result limited.

2) The high LET (~ 40 keV/mm as average [22], or even higher [23]) and very high RBE (≅16 at 2.45MeV) values of fast neutrons should result advantageous for treating radioresistant tumours that require superior dose conformity, by reducing the integral dose and sparing surrounding healthy tissues and critical organs, thus minimizing treatment-related complications and presumably reducing the risk of radiation-induced secondary malignancies (RISMs [41]). Indeed, some pre-clinical studies suggest that DNA ends of DNA damage induced by high-LET IR are more prone to end processing compared to DNA ends of DNA damage induced by low-LET IR. Thus, the nIORT® technique could be very efficient,

even whether the underpinning radio-biological mechanisms are not still fully understood and there is significative amount of data at the biochemical level concerning the IR effects due to accelerator-produced charged particles, as protons and heavy ions, but few data concerning the effects due to high-LET beams of fast neutrons. Nevertheless, the neutron radiobiology experiments clearly identified a higher cell kill per unit dose and an accompanying reduction in oxygen dependency [37].

3) A concurrent effect that could limit the IORT treatment efficacy is represented by so called radiation-induced bystander effect (RIBE), that increase the cell death beyond that which would be predicted (i.e., when tested directly in cultured tumour cell populations, the radiation-induced death models for normal and cancer cells are very complex). But some preclinical studies put in evidence that the RIBE is not induced by neutrons and thus a lower risk for RISMs should occur [42]. Additionally, thanks to the epithermal and thermal tails of the neutron flux spreading out around the tumour bed, the nIORT® could lead to the potential appearance of the radiation induced abscopal effect (RIAE) on distant non-irradiated cells due to the adaptive immune system [43].

4) The high LET-RBE neutrons could also inhibit radically the tumour cell proliferation, as well as their epithelial-mesenchymal transformation (EMT) and transcriptional regulation: if verified, this feature would be fundamental since EMT represents a crucial process endowing the cancer cells with invasive and metastatic properties. Analyses of tumour cavity wound fluids after IORT in breast cancer patients indicates encouraging results: although representing a different TME, the immune microenvironment of glioma in brain cancers has been hypothesized also to play a role in potential IORT effects beyond radiation-induced DNA damage [44,45].

Besides the effectiveness of high LET-RBE neutrons in DNA damaging, in principle the nIORT® technique could extend the IORT applicability beyond the "focused beam" IOERT and "small target volume" IOHDR and, to the same extent, LEX-IORT techniques. The almost-isotropic irradiation field of fast neutrons is well suitable for irradiating tumour bed margins in irregular surfaces and acts as a sort of ionizing radiation "foam" filling the surgical cavity (see Figure 7). The radiation "foam" should allow to induce necrosis and apoptosis of the QCCs within the topography irregularities of the tumour bed and, maybe also overcome their radio-resistance (responsible of multistage cancer progression and cancer metastasis too). Even in absence of clinical evidence, it is possible to argue that - thanks the near-isotropic beam - the nIORT® could result well suitable for large target areas and irregular surfaces, without the precise alignment required by IORT devices with focused beams. Furthermore, for extended tumour beds, it should not require the knowledge of the status of the surgical margins and lymph nodes before the treatment, as in standard IORT techniques.

Despite being a departure from the fractionated schemes of the EBRT, the nIORT® could potentially satisfy all five R's criteria of RT, namely: radiosensitivity, reassortment, repopulation, reoxygenation and repair [46]. The high LET-RBE neutrons are very effective against the cancer cells radio-sensitivity and the repopulation of residual local recurrences in the TME is not present in IORT treatments (thanks to the time to initiation zeroing). The reassortment due to the rapid cells proliferation over the cycle between daily fractioned EBRT irradiations - in which the heterogeneity in cell cycle kinetics re-distributes (reassorts) cancer cells - does not play a role in a single-dose IORT administered immediately after surgery. The reoxygenation effects needed to fix DNA damage (i.e., cancer cells are much more resistant to IR in hypoxic conditions) are also enhanced by the IORT modality. For what concerns the cells repair, the following two main aspects can be observed.

a. The high LET-RBE neutrons induces highly localized DSBs and clustered DNA damage more difficult to repair than SSBs induced by low LET radiation, as photons and electrons. The size and complexity of DNA lesions inflicted by the IR determine how the cells will be repaired counterbalancing the irradiation effects by DSB-repair pathways, such as the nonhomologous end joining (NHEJ) and the homologous recombination (HR). Mostly, the NHEJ pathway plays a predominant role in repairing SSBs induced by low-LET radiation, while the slow DSB repair process that follows exposure to high-LET radiation is mediated by the "less efficient" HR process [47,48,49].

b. While the number of lethal DNA lesions for cancer cells (as DSBs and more complex lesions) is proportional to dose, the repair system of cancer cells becomes saturated at higher dose levels beyond the dose range normally studied in vitro [50]. As emerged from some trials, the DNA of cancer cells repairs more slowly after RT treatments which produce also more DNA breaks (single and double) than in normal cells: in fact, various proteins involved in cell death and DNA damage mechanisms decrease the radio-resistance of the fast-doubling cancer cells, while increase the radio-resistance of slow doubling normal cells [38,51].

Thus, thanks to the high cells radiosensitivity to high LET-RBE fast neutrons and the limitation of the cancer cells repair, the nIORT® treatment could also induce the killing of the motile cancer or metastatic stem cells infiltrating the tumour bed, while X-rays and electrons with lower LET-RBE cannot lead to cells necrosis and, in some cases, induce these cells to develop radio-resistance.

It can be finally remarked that nowadays investigations are exploring the adjuvant combination of immunotherapy and RT. The immune system can modulate either tumour suppression or progression, while RT has the potential to regulate immune responses to yield antitumorigenic effects leading to the LTC [52]. Even if it is still an open arena of research, some clinical evidence [53-56] demonstrated that RT administered to oncological patients might augment the anti-tumour effects of administered immune-checkpoints inhibitors (ICIs). The author's hypothesis is that these anti-tumour effects could also be obtained - and hopefully enhanced - with the CNG-nIORT® deviceadopting high LET-RBE neutrons, by increasing the immune modulatory effect through the stimulation of adaptive and innate immune reactions of the oncological patients. Thus, in conjugation with the ICIs, the nIORT® could trigger a strengthen antitumor response and an improved patient survival.

Concluding Remarks

Despite the prospective outcome data are still limited, the IORT advantages (due to the instant prevention of tumor regrowth, optimized dose-sparing of adjacent healthy tissues and immediate completion of metastases treatment) are nowadays considered comparable - and even superior, when applied in the optimal setting - with the long-term outcomes of adjuvant EBRT. The fast neutron beam of the CNG-nIORT® device could further enhance the eligibility of IORT treatments for solid cancers, e.g., as the brain and breast tumours here considered. The authors' idea is that the nIORT® technique could extend the IORT applicability beyond the current technologies - relying on "focused beam" (IOERT) and "small target volume" (IOHDR and, at same extent, LEX-IORT) devices - mainly because of:

i) the reduced OER, the high LET and very high RBE of fast neutrons (≅16, that should be very effective in cancer cells killing).

ii) the diffuse spatial dose distribution in the irradiated tissues, well suitable also for extended and irregular tumour bed targets.

The neutron beam acts as a sort of ionizing radiation "foam" filling the surgical cavity, by irradiating the tumour bed margins (normally filled by potential QCCs) with lower (but still significant) dose levels, by potentially improving LTC through the reduction of local recurrences and metastasis in the TME. Thus, potentially, the nIORT® technique could be adopted even without the adjuvant administration of chemo-therapeutic alkylating agents, but it could be explored whether the addition of concurrent and adjuvant e.g., temozolomide (TMZ) for brain tumours [57] could mitigate the resistance of the most severe gliomas and their function in the TME.

Besides the benefits due to the peculiar "physical-biological" features of fast neutrons, accurate simulations with the MCNP code - modelling the CNG equipped with 4-cm-diameter nIORT® applicators inserted in the breast and brain surgical cavities - demonstrated that:

a) an almost iso-dose rate spatial distribution of ≅2 Gy (RBE)/min can be administered with the hemispherical applicator in the breast tumor bed;

b) a more front-focused dose rate distribution can be administered with the cylindrical applicator in the brain surgical cavity (with craniotomy). The peak of about ≅5 Gy (RBE)/min is delivered in the tumour bed centre and significantly lower values (≅1.5 Gy (RBE)/min) in the surrounding brain, skull and skin normal tissues.

Therefore, with both applicators the CNG-nIORT® device could administer the clinical endpoints foreseen by the standard IORT protocols (~10-20 Gy (RBE)) in a one-shot irradiation of few minutes. Additionally, the possible choice of different nIORT® applicator shape (and size) - that lead to different spatial dose distributions - should allow a proper balancing between the aimed local control of the tumour and the adverse effects of the radiation on normal tissues, as required in common clinical practice for the selection of the most suitable treatment.

The potential cytotoxicity of the neutron radiation field should be avoided thanks to the very limited open airspace between the applicator and the surgical resection cavity during the nIORT® treatment.

The MCNP results here reported deals only with the radiological aspects associated with the nIORT® irradiation of (head and trunk) human tissues and are not related to the specific cancer pathology. At the same time, the values of the main therapeutic parameters obtained could be generalized for the treatment of other body parts: for more accurate dose levels and spatial distributions, the topography of the specific organs/tissues of the surgical cavity should be properly modelled.

Acknowledgements

The authors acknowledge the expert assistance and collaboration of the TC, ENEA, and BT colleagues. The computing resources for this work have been provided by CRESCO/ENEAGRID High Performance Computing infrastructure (funded by ENEA and by Italian and European research programs) and its staff (see *http://www.cresco.enea.it* for information).

References

1. Vignard J, Mirey G, Salles B (2013) Ionizing-radiation induced DNA double-strand breaks: a direct and indirect lighting up. Radiother. Oncol 108(3): 362-9.
2. Hensley FW (2017) Present State and Issues in IORT Physics. Radiat Oncol 12(1): 37.
3. Hashemi S (2021) Comparison of IORT (Radical and Boost Dose) and EBRT in Terms of Disease-Free Survival and Overall Survival according to Demographic, Pathologic, and Biological Factors in Patients with Breast Cancer. J. of Surgical Oncology 2476527.
4. Williams NR, Pigott KH, Brew-Graves C, Keshtgar MR (2014) Intraoperative radiotherapy for breast cancer. Gland Surg. 3(2): 109-119.
5. Cifarelli CP, Jacobson GM (2021) Intraoperative Radiotherapy in Brain Malignancies: Indications and Outcomes in Primary and Metastatic Brain Tumors. Front. Oncol. Sec. Radiation Oncology 11: 768168.
6. Giordano FA, Abo-Madyan Y, Brehmer S, Herskind1 C, Sperk E, et al. (2014) Intraoperative radiotherapy (IORT) - a resurrected option for treating glioblastoma? Translational Cancer Research 3(1).
7. Wu W, Klockow JL, Zhang M, Lafortune F, Chang E, et al. (2021) Glioblastoma multiforme (GBM): an overview of current therapies and mechanisms of resistance. Pharmacol Res 171: 105780.
8. Sethi A, Emami B, Small WJ, Thomas TO (2018) Intraoperative Radiotherapy With INTRABEAM: Technical and Dosimetric Considerations. Frontiers in Oncology 8:74.
9. Usychkin S, Calvo F, Dos Santos MA, Sambas J, De Urbina DO, et al. (2013) Intra-Operative Electron Beam Radiotherapy for Newly Diagnosed and Recurrent Malignant Gliomas: Feasibility and Long-Term Outcomes. Clin. Transl. Oncol 15(1).
10. Severgnini M, De Denaro M, Bortul M, Vidali C, Beorchia A (2014) In vivo dosimetry and shielding disk alignment verification by EBT3 GAFCHROMIC film in breast IOERT treatment. Appl. Clin. Med. Phys 16(1): 5065.
11. Chitti B, Goyal S, Sherman JH, Caputy A, Sarfaraz M, et al. (2020) The role of brachytherapy in the management of brain metastases: a systematic review. Contemp. Brachytherapy 12(1): 67-83.
12. Cifarelli CP, Brehmer S, Vargo JA, Hack JD, Kahl KH, et al. (2019) Intraoperative Radiotherapy (IORT) for Surgically Resected Brain Metastases: Outcome Analysis of an International Cooperative Study. Neurooncol 145(2): 391-397.

13. Giordano FA, Brehmer S, Mürle B, Welzel G, Sperk E, et al. (2019) Intraoperative Radiotherapy in Newly Diagnosed Glioblastoma (INTRAGO): An Open-Label, Dose-Escalation Phase I/II Trial. Neurosurgery 84(1): 41-49.

14. Marthinsen AB, Gisetstad R, Danielsen S, Frengen J, Strickert T, et al. (2010) Relative Biological Effectiveness of Photon Energies Used in Brachytherapy and Intraoperative Radiotherapy Techniques for Two Breast Cancer Cell Lines. Acta Oncol 49(8): 1261-1268.

15. Jones B (2021) Fast neutron energy based modelling of biological effectiveness with implications for proton and ion beams. Phys. Med. Biol 66(4): 045028.

16. Baiocco G, Barbieri S, Babini G, Morini J, Alloni D, et al. (2016) The origin of neutron biological effectiveness as a function of energy. Scientific Reports 6: 34033.

17. Bleddyn J (2020) Clinical Radiobiology of Fast Neutron Therapy: What Was Learnt? J. Front. Oncol. Sec. Radiation Oncology 10: 1537.

18. Martellini M, Gherardi G (2019) Apparatus for intraoperative radiotherapy. European Patent 11(3).

19. Leung KG (2020) New compact neutron generator system for multiple applications. Nuclear Technology 206(10): 1-8.

20. Martellini M, Sarotto M, Leung K, Gherardi G (2023) A Compact Neutron Generator for the nIORT® Treatment of Severe Solid Cancers. Medical Research Archives 11(3).

21. (2018) Laboratorio per la caratterizzazione di Irradiatori Neutronici Compatti in Emilia Romagna. LINCER project funded by Emilia Romagna with "Legge Regionale 27/12/2018 N.25, DGR N. 545/2019 - CUP I74I19000360003".

22. Dousset MH, Hamard J, Ricourt A (1971) Distribution of the dose from neutrons in a thin sample of wet tissue as a function of linear energy transfer (LET). Phys. Med. Biol 16(3): 467-478.

23. Krüll A, Schwarz R, Brackrock S, Engenhart-Cabillic R, Huber P, et al. (1998) Neutron Therapy in Malignant Salivary Gland Tumors: Results at European Centers. Engenhart-Cabillic R, Wambersie A. (eds) Fast Neutrons and High-LET Particles in Cancer Therapy. Recent Results in Cancer Research 150: 88-99.

24. (2007) Annals of the International Commission on Radiological Protection. ICRP 103(37).

25. Antonovic L, Lindblom E, Dasu A, Bassler N, Furusawa Y, et al. (2014) Clinical oxygen enhancement ratio of tumors in carbon ion radiotherapy: the influence of local oxygenation changes. Radiation Research 55(5): 902-911.

26. Rini F, Hall EJ, Marino SA (1979) The Oxygen Enhancement Ratio as a Function of Neutron Energy with Mammalian Cells in Culture, Radiation Research 78(1): 25-37.

27. Nishitani T, Yoshihashi S, Tanagami Y, Tsuchida K, Honda S, et al. (2022) Neutronics Analyses of the Radiation Field at the Accelerator-Based Neutron Source of Nagoya University for the BNCT Study. Elsevier Nucl. Eng 3(3): 222-232.

28. Tillery H, Moore M, Gallagher KJ, Taddei PG, Leuro E, et al. (2022) Personalized 3D-printed anthropomorphic whole-body phantom irradiated by protons, photons, and neutrons. Biomed. Phys. Eng. Express 8(2).

29. Pelowitz B (2013) MCNP6 user's manual. Tech. Rep. Los Alamos National Lab.

30. Martellini M, Gherardi G, Leung K, Leung JK, Sarotto M, et al. (2023) Multi-Purpose Compact Apparatus for the Generation of a high flux of neutrons, particularly for Intraoperative Radiotherapy. Int. Patent 2021; PCT/IT2021/000032. WIPO (World Intellectual Property Organisation).

31. Sarotto M (2021) Parametric MCNP analyses to address the design of a neutron collimator for high-flux compact DD sources to be used in cancer radiotherapy. Tech Rep ENEA SICNUC-P000-044.

32. Sarotto M, Martellini M (2022) MCNP analyses of the 100 kV D-ion-based compact neutron source: irradiation performances for nIORT® treatments with different irradiation window diameters. Tech Rep ENEA SICNUC-P000-045.

33. Martellini M, Sarotto M, Leung K, Gherardi G, Rizzo A, et al. (2024) Feasibility Study on the nIORT® Adjuvant Treatment of Glioblastoma Multiforme through the Irradiation Field of Fast Neutrons Produced by a Compact Generator. Medical Research Archives 12(2).

34. Obložinský P (2018) Special Issue on Nuclear Data. Nuclear Data Sheets 148: ISSN: 0090-3752.

35. Kramer R, Zankl M, Williams G, Drexler G (1982) The calculation of dose from external photon exposures using reference human phantoms and Monte-Carlo: part I. The male (Adam) and female (Eva) adult mathematical phantom. Tech Report GSF S-885 (Germany).

36. Pilar A, Gupta M, Laskar SG, Laskar S (2017) Intraoperative radiotherapy: review of techniques and results. cancer medical science 11(750).

37. Niemantsverdriet, Van Goethem MJ, Bron R, Hogewerf W, Brandenburg S, et al. (2012) High and Low LET Radiation Differentially Induce Normal Tissue Damage Signals. Int. J. Radiation Oncol. Biol. Phys 83(4): 2791-2797.

38. Baskar R, Dai J, Wenlong N, Yeo R, Yeoh KW (2014) Biological response of cancer cells to radiation treatment. Frontiers in Molecular Biosciences 1:24.

39. (2001) International Atomic Energy Agency. Current status of neutron capture therapy IAEA TECDOC-1223.

40. Seneviratne D, Advani P, Trifiletti DM, Chumsri S, Beltran CJ, et al. (2022) Exploring the Biological and Physical Basis of Boron Neutron Capture Therapy (BNCT) as a Promising Treatment Frontier in Breast Cancer. Cancers 4(12): 3009.

41. Busato F, ElKhouzai B, Mognato M (2022) Biological Mechanisms to Reduce Radioresistance and Increase the Efficacy of Radiotherapy: State of the Art. Int. J. of Molecular Science 23(18): 10211.

42. Wang C, Smith RW, Duhig J, Prestwich WV, Byun SH, et al. (2011) Neutrons do not produce a bystander effect in zebrafish irradiated in vivo. Int. J. Radiat. Biol 87(9): 964-973.

43. Trivillin VA, Pozzi EC, Colombo LL, Thorp SI, Garabalino MA, et al. (2017) Abscopal effect of boron neutron capture therapy (BNCT): proof of principle in an experimental model of colon cancer. Radiat. Environ. Biophys 56(4): 365-375.

44. Gapanova AV, Rodin S, Mazina AA, Volchkov V (2020) Epithelial-Mesenchymal Transition: Role in Cancer Progression and the Perspectives of Antitumor Treatment. Acta Naturae 12(3): 4-23.

45. Roche J (2018) The Epithelial-to-Mesenchymal Transition in Cancer. Cancers 10(2): 52.

46. Herskind C, Ma L, Liu Q, Zhang B, Schneider F, et al. (2017) Biology of high single doses of IORT: RBE, 5 R's, and other biological aspects. Radiation Oncology 2(1):24.

47. Shibata A, Conrad S, Birraux J, Geuting V, Barton O, et al. (2011) Factors determining DNA double-strand break repair pathway choice in G2 phase. EMBO Journal (European Molecular Biology Organization) 30(6):1079-1092.

48. Mladenova V, Mladenov E, Chaudhary S, Stuschke M, Iliakis G (2022) The high toxicity of DSB-clusters modelling high-LET-DNA damage derives from inhibition of c-NHEJ and promotion of alt-EJ and SSA despite increases in HR. Frontiers in Cell and Developmental Biology 10: 1016951.

49. Mahaney BL, Meek K, Lees Miller SP (2009) Repair of Ionizing radiation-induced DNA double strand breaks by non-homologous end-joining. Biochemical J 417(3): 639-650.

50. Van de Kamp G, Heemskerk T, Kanaar R, Essers J (2021) DND Double

Strand Break Repair Pathways in response to different types of ionizing radiation. Frontiers in Genetics, Sec. Human and Medical Genomics 12: 738230.

51. Baskar R, Lee KA, Yeo R, Yeoh KW (2012) Cancer and radiation therapy: current advances and future directions. Int J Med Sci 9(3): 193-199.

52. Kumari S, Mukherjee S, Sinha D, Abdisalaam S, Krishnan S, et al. (2020) Immunomodulatory Effects of Radiotherapy. Int. J. of Molecular Sciences 21(21): 8151.

53. Chi A, Nguyen N P (2023) Mechanistic rationales for combining immunotherapy with radiotherapy. Front. Immunol 14: 1125905.

54. Awada H, Paris F, Pecqueur (2023) Exploiting radiation immunostimulatory effects to improve glioblastoma outcome. Neuro-Oncology 25(3): 433-446.

55. Gillette JS, Wang JE, Dowd RS, Toms SA (2023) Barriers to overcoming immunotherapy resistance in glioblastoma. Front. Med 10: 1175507.

56. Layer JP, Shiban E, Brehmer S, Diehl CD, Guedes de Castro D, (2024) Multicentric assessment of safety and efficacy of combinatorial adjuvant brain metastasis treatment by intraoperative radiotherapy and immunotherapy. Int J of Radiation Oncology Biology Physics.

57. Singh N, Miner A, Hennis L, Mittal S (2021) Mechanisms of temozolomide resistance in glioblastoma-a comprehensive review. Cancer Drug Resist 4(1): 17-43.